



Multivariate analysis of near additions for presbyopic patients at a rural optometry clinic

Authors:

Khisimusi D. Maluleke^{1,2}
Nabeela Hasrod¹
Alan Rubin¹

Affiliations:

¹Department of Optometry,
Faculty of Health Science,
University of Johannesburg,
Johannesburg, South Africa

²Limpopo Department of
Health, Polokwane,
South Africa

Corresponding author:

Khisimusi Maluleke,
kdebree@yahoo.com

Dates:

Received: 25 July 2024
Accepted: 07 Jan. 2025
Published: 28 Feb. 2025

How to cite this article:

Maluleke KD, Hasrod N,
Rubin A. Multivariate analysis
of near additions for
presbyopic patients at a rural
optometry clinic. *Afr Vision
Eye Health*. 2025;84(1), a980.
[https://doi.org/10.4102/
aveh.v84i1.980](https://doi.org/10.4102/aveh.v84i1.980)

Copyright:

© 2025. The Author(s).
Licensee: AOSIS. This work
is licensed under the
Creative Commons
Attribution License.

Read online:



Scan this QR
code with your
smart phone or
mobile device
to read online.

Background: Presbyopia is often overlooked in refractive error distribution analysis. This article employs multivariate analysis to address this gap, enhancing understanding of means, outliers and variations through graphical data presentation.

Aim: To analyse the distribution of near-corrective optical additions for presbyopic patients over 2 years at a rural optometry clinic.

Setting: The study was conducted at Sekororo District Hospital, South Africa.

Methods: Non-cycloplegic near-refractive error data for presbyopic patients who visited the clinic at the district hospital from January 2018 to December 2019 were extracted from the hospital's records. The records were randomly divided into two groups for 2018 and 2019. Meridional plots and stereo-pair scatter plots were used to analyse the refractive states for the right (OD) and left (OS) eyes.

Results: In the 2018 sample, the clinical means for OD and OS were $+1.33 -0.32 \times 90$ and $+2.01 -0.37 \times 77$, respectively. Similarly, for the 2019 sample, the clinical means for OD and OS were $+2.01 -0.32 \times 82$ and $+1.82 -0.18 \times 95$, respectively. The data were not normally distributed, and outliers were present. Sample variances were spherical rather than astigmatic.

Conclusion: Deviation from the normality showed that the data for OD and OS were mainly mildly positively skewed. Much of the variation in the refractive state was spherical (the stigmatic) irrespective of the laterality.

Contribution: The article makes a valuable contribution to the current understanding of multivariate analysis, in academic training including optometry fraternity, as it pertains to the refractive state of the eyes in a rural optometry clinic.

Keywords: dioptric power; refractive errors; presbyopia; near-vision impairment; distributional analysis.

Introduction

Presbyopia is a very common age-related vision disorder recognised by decreased physiological accommodation of the eye, leading to blurred near-vision in the absence of optical or surgical compensation.^{1,2,3,4} As people age, especially adults aged 35 years or older, their eyes' ability to adjust declines. In addition, presbyopia is often defined as an inability to read N8 at 40 cm.^{4,5} Uncorrected presbyopia can lead to near-vision impairment (NVI), which presents significant economic and personal challenges in daily activities that require close visual focus, such as reading fine print and working on computer screens.^{1,2} Economically, uncorrected presbyopia can reduce industrial productivity, as the affected adult workers may struggle to read product labels efficiently.⁴

As per global published data from 2015 to date, approximately 1.8 billion people (with an estimated prevalence of 25%) have presbyopia, which leaves 826 million people affected by NVI.¹ In the sub-Saharan African region, unaddressed presbyopia is the second major cause of NVI after cataracts.^{1,4} In this region, about 48.5% of moderate-to-severe cases of NVI are caused by uncorrected presbyopia. However, the prevalence varies among the studies and regions in Africa. For instance, in Enugu State in north-eastern Nigeria, it is 63.4%.⁵ In Kwara State, Nigeria, the prevalence is 59.7%.⁶ Meanwhile, in the KwaZulu-Natal province in South Africa, the prevalence of presbyopia is reported to be 77.0%.⁷ Limpopo province, South Africa, has a 28.1% prevalence of moderate-to-severe vision impairments reported in 29 public hospitals, primarily because of uncorrected refractive errors, including presbyopia.⁸

The near- or proximal refractive errors for presbyopic patients are usually recorded with near additions. Clinical notations of the sphere (F_s), cylinder (F_c), and the corresponding axis (A) of the cylinder and the near addition (F_{add}) must be transformed into dioptric power matrices or vectors for effective scientific analysis using Matlab software.^{9,10,11,12,13,14,15,16} This allows the sphero-cylinders to be statistically analysed as one entity for univariate or multivariate methods to be used with near-refractive errors and quantitative information (with statistical measures) such as the means, standard deviations or variances to become measurable. The article published by Harris¹⁶ shows a proper representation of near-refractive errors, including three-dimensional (3D) surfaces of constant probability density with stereo-pairs scatter plots in 3D Euclidean symmetric dioptric power spaces. Other quantitative analyses of near-refractive errors for presbyopic patients in two-dimensional spaces include meridional profiles of dioptric power and other methods that will be used herein.¹⁶ Using these methods, the distributions of near-refractive errors for the right (OS) and left (OS) eyes can be more easily investigated, properly analysed and better understood.^{14,16,17,18,19}

This article highlights the importance of employing advanced scientific methodologies, specifically multivariate analysis, to comprehensively understand the prescribing patterns of the near-optical additions for presbyopic individuals. The findings derived from this analysis are anticipated to enhance clinical decision-making processes related to the provision of presbyopic corrections. It is expected to be readily comprehensible to professionals across various scientific disciplines. Furthermore, this method helps identify trends specific to the population, even if they seem unrelated to rural areas, such as Limpopo province, South Africa. In this province, access to ophthalmic care is often limited. Limpopo has an estimated population of approximately 6 million dwellers who face three major challenges: poverty, unemployment and inequality.²⁰ These issues can result in an undersupply of optical corrections for presbyopia, such as spectacles, as many dwellers lack medical insurance (such as a medical aid scheme) to access private healthcare.²⁰ Consequently, they depend on public healthcare facilities. This information is based on recent data published by Statistics South Africa (SSA).²⁰

This study aims to analyse near-refractive errors in presbyopic patients using multivariate methods to gain insights into their distribution and variability. The results will inform the development of tailored interventions designed to enhance near-vision corrections in rural communities in South Africa and elsewhere.

Research methods and design

Study design and setting

This cross-sectional study used historical records from the clinical archive to save time and reduce the costs of research materials. Subjective refraction data were collected retrospectively for presbyopic patients who visited the

optometry clinic at Sekororo District Hospital in Limpopo, South Africa, from 2018 to 2019. This hospital is the only facility in the rural Maruleng sub-district providing secondary healthcare including eye care offered by one optometrist and two ophthalmic nurses, with referrals to Mankweng Hospital for ophthalmologist care.

Sampling

The clinical archive of the selected district hospital contained 1140 records. Of these, 627 records were excluded because of missing important information, resulting in 513 usable records – about 134% more than the required sample size (384) calculated using the statistical formula of Cochran as shown in Equation 1:

$$n = \frac{Z^2 P(1-P)}{e^2} = \frac{(1.96)^2 0.50(1-0.50)}{(0.05)^2} = 384 \quad [\text{Eqn 1}]$$

where P is the percentage occurrence of refractive errors (P) set at 0.5, assuming 50% of records were presbyopic and 50% non-presbyopic. The margin of error is represented by e , and Z was set at 1.96 for a 95% confidence level. We excluded 262 records lacking near additions for non-presbyopic individuals, resulting in a final sample of 251 presbyopic records: 141 from 2018 and 110 from 2019, used for multivariate analysis methods (see Figure 1). To ensure a representative sample, a probability-stratified random sampling method was applied to the records from 2018 to 2019. This approach was successful in the previously published study by Maluleke et al.²¹ on the distribution of non-cycloplegic refractions where the final sample is more representative, with all the records selected within their respective stratum (for 2018 and 2019). Among the 513 records, 251 were from presbyopic patients and 262 from non-presbyopic patients.

Statistical analysis

The near-refractive error data for presbyopic patients were recorded in the pivot tables of an Excel spreadsheet (Microsoft 365) and then imported into Matlab software (The MathWorks, US). In Matlab, near-refractive errors were converted from clinical data into dioptric power matrices for further analysis to address the primary objective of this study using multivariate analysis methods to examine the distribution of near-refractive errors in a rural setting. The analysis will also incorporate the means (namely, the clinical and matrix/component means), variance-covariances, meridional profiles and stereo-pairs with surfaces of constant density (or distribution ellipsoids).^{14,15,16,18,19,20,21,22,23,24,25,26,27,28,29,30,31,32,33,34,35,36} Following is a detailed illustration of near-refractive error data conversions, including the purpose of the respective methods used in this study.

Dioptric power matrices and analysis for distributions of refractive errors

Dioptric power matrices (DPM) for an effective scientific analysis are included herein (Equation 2) as the transformation of near-refractive errors for presbyopic patients

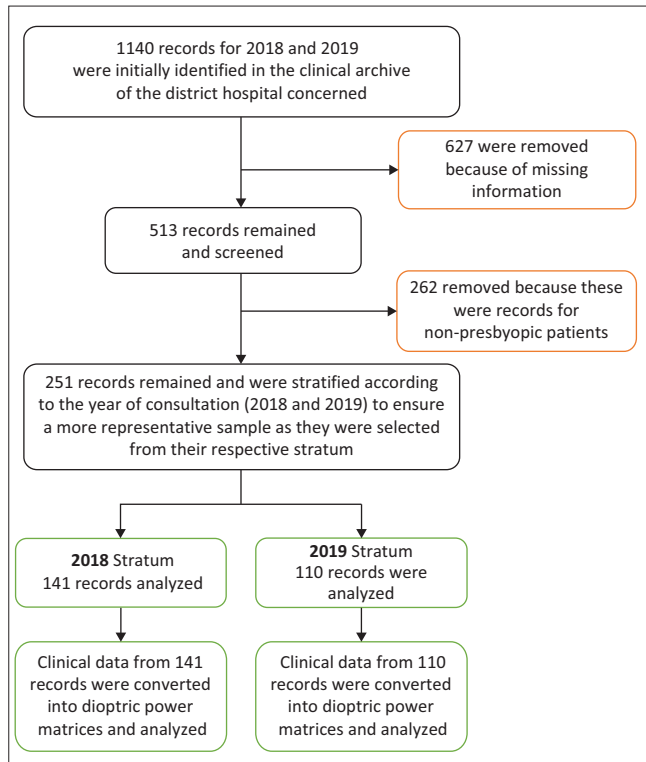


FIGURE 1: Flowchart on extraction, exclusion and inclusion, and analysis.

from clinical notations ($S C A$ or $F_s F_c A$) to 2×2 symmetric power matrices \mathbf{F} (or vectors, \mathbf{f} or others) and scientific analysis of dioptric power has been previously described in detail^{9,10,11,12,13,14,15,16,17,18,19,21,22,23,24,25,26,27,28,29,30,31,32,33,34,35,36}.

$$\mathbf{F} = \begin{pmatrix} f_{11} & f_{12} \\ f_{21} & f_{22} \end{pmatrix} = \begin{pmatrix} F_s + F_c \sin^2 A & -F_c \sin A \cos A \\ -F_c \sin A \cos A & F_s + F_c \cos^2 A \end{pmatrix} \text{m}^{-1} \text{ or D} \quad [\text{Eqn 2}]$$

Note that f_{11} and f_{22} in Equation 2 are (curvital) powers in the horizontal and vertical meridians, respectively, while $f_{12} = f_{21}$ are (torsional) powers in the reference meridian (typically horizontal, but not always). Cylinders in ophthalmology and optometry are measured, of course, for the horizontal meridian.

From clinical notation or \mathbf{F} , Equation 3 can be used for the scalar and anti-scalar (or anti-stigmatic) coefficients of power (see vector \mathbf{f} [from Harris] or \mathbf{t} [from Thibos et al.]¹⁹):

$$\mathbf{f} = \begin{pmatrix} F_I \\ F_J \\ F_K \end{pmatrix} = \begin{pmatrix} \frac{1}{2}(f_{11} + f_{22}) \\ \frac{1}{2}(f_{11} - f_{22}) \\ \frac{1}{2}(f_{21} - f_{12}) \end{pmatrix} = \begin{pmatrix} F_s + 0.5F_c \\ -0.5F_c \cos 2A \\ -0.5F_c \sin 2A \end{pmatrix} = \begin{pmatrix} M \\ J_0 \\ J_{45} \end{pmatrix} = \mathbf{t} \quad [\text{Eqn 3}]$$

The quantities M , J_0 and J_{45} in Equation 3 for Thibos et al.¹⁹ are equivalent to the stigmatic coefficient (F_I) ortho-anti-stigmatic coefficient (F_J) and the oblique anti-stigmatic coefficient (F_K).^{21,32} The scalar or stigmatic ($F_I = M$) coefficient is essentially the spherical equivalent (SE) or nearest sphere (F_{ns}), while the term anti-scalar (antistigmatic or 'Jacksonian') refers to powers represented by Jackson Cross Cylinders (JCC). It is important to note that for the asymmetric power matrices (where $f_{12} \neq f_{21}$ in Eqn 2), there is another vector element (F_L) that is ignored here. Thus, $M = F_I$, $J_0 = F_J$, and $J_{45} = F_K$ and these coefficients are used, respectively, with the basis matrices \mathbf{I} , \mathbf{J} and \mathbf{K} , namely $\begin{pmatrix} 1 & 0 \\ 0 & 1 \end{pmatrix}$, $\begin{pmatrix} 1 & 0 \\ 0 & -1 \end{pmatrix}$ and $\begin{pmatrix} 0 & 1 \\ 1 & 0 \end{pmatrix}$ for representation using stereo-pairs plots. The 3×3 symmetric variance-covariance matrix \mathbf{S}_{ff} from Equation 4 to Equation 5 provides the necessary variances and covariances for distributions of refractive errors:

$$\mathbf{S}_{ff} = \frac{1}{n-1} \sum_{i=1}^N (\mathbf{f}_i - \bar{\mathbf{f}})(\mathbf{f}_i - \bar{\mathbf{f}})^T \quad [\text{Eqn 4}]$$

and

$$\mathbf{S}_{ff} = \begin{pmatrix} S_{II} & S_{IJ} & S_{IK} \\ S_{JI} & S_{JJ} & S_{JK} \\ S_{KI} & S_{KJ} & S_{KK} \end{pmatrix} \mathbf{D}^2 \quad [\text{Eqn 5}]$$

where S_{II} is the stigmatic variance, S_{IJ} and S_{KK} are ortho-anti-stigmatic and oblique anti-stigmatic variances, respectively, while $S_{IJ} (= S_{JI})$ is the stigmatic ortho-anti-stigmatic covariance, $S_{IK} (= S_{KI})$ is the stigmatic and oblique anti-stigmatic covariance and $S_{JK} (= S_{KJ})$ is the ortho- and oblique anti-stigmatic covariance. Given that \mathbf{S}_{ff} is symmetrical, only six entries are distinct; variances are always positive, but covariances can be positive or negative. Means, variances and covariances are essential statistics for distributions of refractive errors, and Equation 6 is the sample mean:

$$\bar{\mathbf{f}}_i = N^{-1} \sum_{i=1}^N \mathbf{f}_i \quad [\text{Eqn 6}]$$

where N is the sample size and vector \mathbf{f} with index $i = 1$ to N is used.

The normality of refractive error distributions is assessed using meridional or polar profiles with univariate Mardia's skewness (β_1) and kurtosis (β_2). The expected skewness (β_1) should be zero for a symmetric or normal data distribution. However, computed values above or below zero are considered positively and negatively skewed, respectively.^{16,19,21,22,23} The expected value of kurtosis (β_2) should be three for mesokurtic distributions of near-refractive errors, with values below or above three considered platykurtic or leptokurtic.^{16,19,21,24}

Figure 1 summarises the workflow for data extraction, exclusion and inclusion criteria, and analysis. Initially, 1140 records were identified from the clinical archive, but after

applying exclusion and inclusion criteria, the final sample included 251 records: 141 from 2018 and 110 from 2019.

Ethical considerations

Ethical approval (reference no.: REC-1170-2021) was obtained from the Research Ethics Committee (REC) in the Faculty of Health Sciences at the University of Johannesburg, South Africa. Permission to conduct the study at the selected district hospital was granted by the Provincial Health Research and Ethics Committee in the Limpopo Department of Health, South Africa, and the Chief Executive Officer of Sekororo District Hospital.

Results

The study had two stratified random samples (2018 and 2019) based on historical records from the clinical archive of the district hospital concerned. The mean ages and standard deviations (\pm s.d.) for the 2018 and 2019 samples were 62.92 ± 10.63 years and 61.92 ± 10.11 years, respectively. The age of presbyopic patients seen at the optometry clinic in 2018 ranged from 42 to 87 years. For those who were seen at the clinic in 2019, their age ranged from 41 to 89 years. Sampled records were of African descent with more females compared to males.

Table 1 shows the statistical output variables of the near-refractive errors for OD and OS of presbyopic patients consulted at the clinic in the 2018 and 2019 samples. Statistics related to near-refractive errors for OD and OS herein are presented in the form of the clinical and component means, norms of the means, variances and covariances, and volumes of 95% ellipsoids.

Figure 2 shows meridional profiles of dioptric powers using Mardia's skewness (β_1) and kurtosis (β_2), aimed at assessing the normality of the near-refractive error data for presbyopic patients consulted at a clinic in 2018 and 2019. For normal distribution, the β_1 profile is expected to be zero, meaning no

skewness but a deviation of the profile above or below zero shows either positive or negative skewing, respectively. Mesokurtosis for a normal distribution is expected to be three (3), with deviations above or below three indicating leptokurtosis or platykurtosis, respectively. Profiles are drawn using different thicknesses to assist readers. Figure 2a shows nearly mesokurtosis ($\beta_2 \approx 3$) for normal distributions for OD (black) and leptokurtosis ($\beta_2 \approx 5$) for OS (red) – see the top thicker profiles for all meridians in h_1 and h_3 curvital powers in the 2018 presbyopic sample. However, the near-refractive error data for presbyopic sample for OD and OS also showed a section of positive or negative skewness ($\beta_1 < 0$ or > 0) for different meridians for h_2 torsional power. Part Figure 2b for the 2019 sample showed leptokurtosis ($\beta_2 > 3$) for both OD (green) and OS (blue) eyes for all meridians in h_1 and h_3 curvital power, and positively and negatively skewed data ($\beta_1 < 0$) for different meridians in h_2 curvital power. Thus, in general, samples here were not normally distributed irrespective of year or laterality (OD or OS).

Kurtosis profiles (β_2) are thicker while skewness profiles (β_1) are thinner.

Figure 2 consists of (Figure 2a) profiles for β_1 and β_2 for 141 near-refractive errors for OD and OS using thick black and red profiles, respectively, for the 2018 sample, (Figure 2b) profiles for β_1 and β_2 for 110 near-refractive errors for OD and OS using thick green and blue profiles, respectively, for the 2019 sample. The shapes and values for the profiles provide information about the samples using Mardia's univariate skewness (β_1) and kurtosis (β_2). The top plots for curvital powers of h_1 and h_3 are set at plus 90 degrees ($+90^\circ$) for β_1 and β_2 in (Figure 2a) and (Figure 2b) for OD and OS, respectively. The two bottom profiles in (Figure 2a) and (Figure 2b) for β_1 and β_2 refer to the torsional powers for h_2 . Reference meridians (in degrees) range from 0° to 180° in 20° intervals. Dashed lines represent the expected values (at 3 and 0) for sample normality. Figure 3 shows stereo-pair scatter plots with 95% distribution ellipsoids for 2018 near-refractive errors ($n = 141$) and 2019 near-refractive

TABLE 1: Statistical output variables for OD and OS of the 2018 and 2019 near-refractive errors.

Samples	n	Eyes	Clinical means (D, D ²)	Component means (D)	Norm of the means (D)	Variances and covariances (D ²)	Volumes of 95% ellipsoids (D ³)
2018	141	OD	$1.33 - 0.32 \times 90$	$1.166I - 0.160J - 0.001K$	1.66	$\begin{pmatrix} 1.796 & -0.058 & 0.012 \\ -0.058 & 0.160 & 0.006 \\ 0.012 & 0.006 & 0.051 \end{pmatrix}$	3.09
		OS	$2.01 - 0.37 \times 77$	$-1.165I - 0.070J + 0.082K$	2.59	$\begin{pmatrix} 1.169 & -0.049 & -0.093 \\ -0.049 & 0.160 & -0.012 \\ -0.093 & -0.012 & 0.084 \end{pmatrix}$	3.05
2019	110	OD	$2.00 - 0.32 \times 82$	$1.839I - 0.151J + 0.046K$	2.61	$\begin{pmatrix} 0.710 & -0.044 & -0.041 \\ -0.044 & 0.135 & 0.011 \\ -0.041 & 0.011 & 0.062 \end{pmatrix}$	2.04
		OS	$1.82 - 0.18 \times 95$	$1.725I - 0.090J - 0.015K$	2.44	$\begin{pmatrix} 1.161 & -0.002 & -0.013 \\ -0.002 & 0.087 & 0.004 \\ -0.013 & -0.004 & 0.032 \end{pmatrix}$	1.46

Note: The variables include clinical and component means, 3×3 variance and covariance matrices in square dioptres, and the volumes of 95% ellipsoids in cubic dioptres for OD and OS. OD, right eye; OS, left eye; D, dioptre.

errors ($n = 110$) for presbyopic patients consulted at the clinic. The data are shown with points for OD and OS. Near-refractive errors were largely stigmatic and shifted in a hyperopic direction because of positive additions to compensate for presbyopia. (Additions for OD and OS were equivalent within participants, that is, unequal additions were not prescribed to any patient.) There are few data points outside the ellipsoids in Figure 3a, b, c and d. Variation was mainly stigmatic and there were a few outliers outside the ellipsoids.

Figure 3 presents presbyopic samples for (Figure 3a) 2018 OD (black), (Figure 3b) 2018 OS (red), (Figure 3c) 2019 OD (green) and (Figure 3d) 2019 OS (blue). The axis lengths are 5 D or 5I D with tick intervals of 1 D. The origin of the axes is at zero dioptres (0 D). The stigmatic axis (labelled 5I) represents spherical powers, while labels 5J and 5K indicate the ortho-anti-stigmatic and oblique anti-stigmatic axes, respectively.

Figure 4 presents stereo-pair plots with 95% confidence ellipsoids (CE) on the mean near-refractive errors for OD and

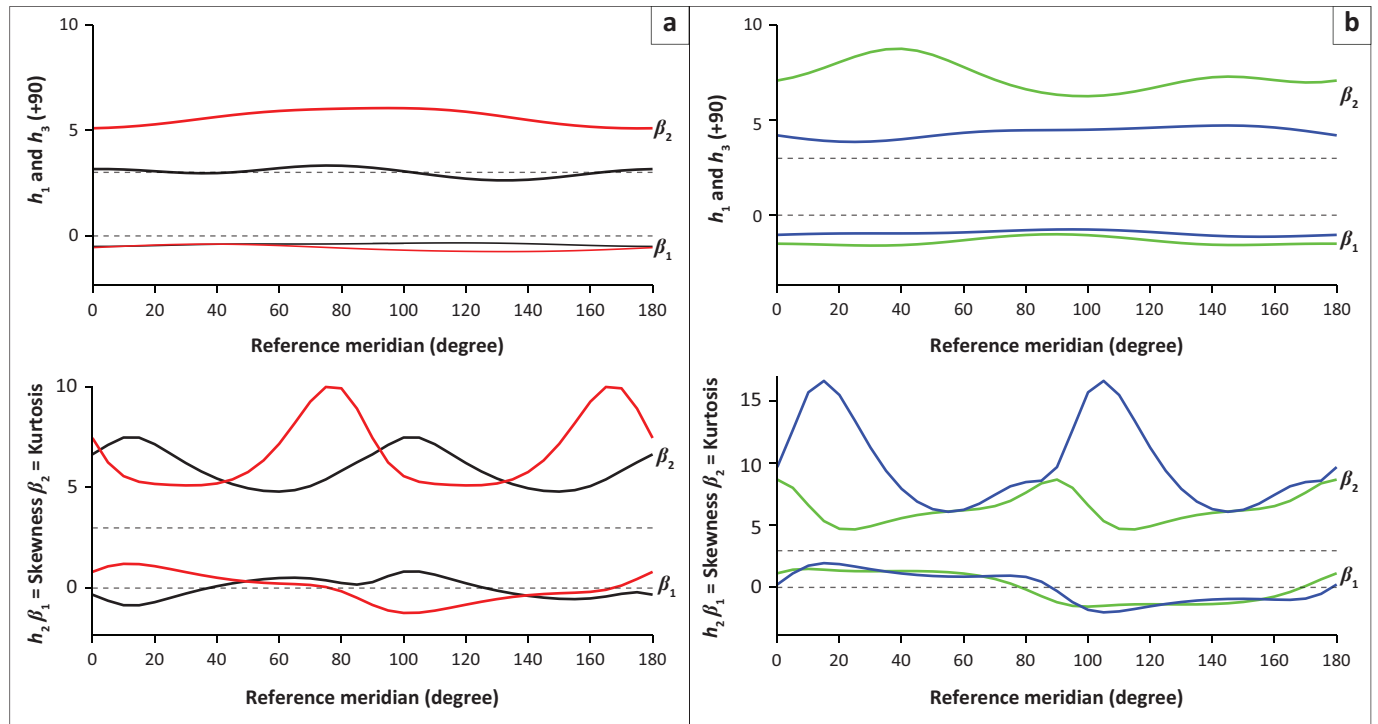


FIGURE 2: (a–b) Meridional profiles for the right and left near-refractive errors in the 2018 and 2019 presbyopic samples.

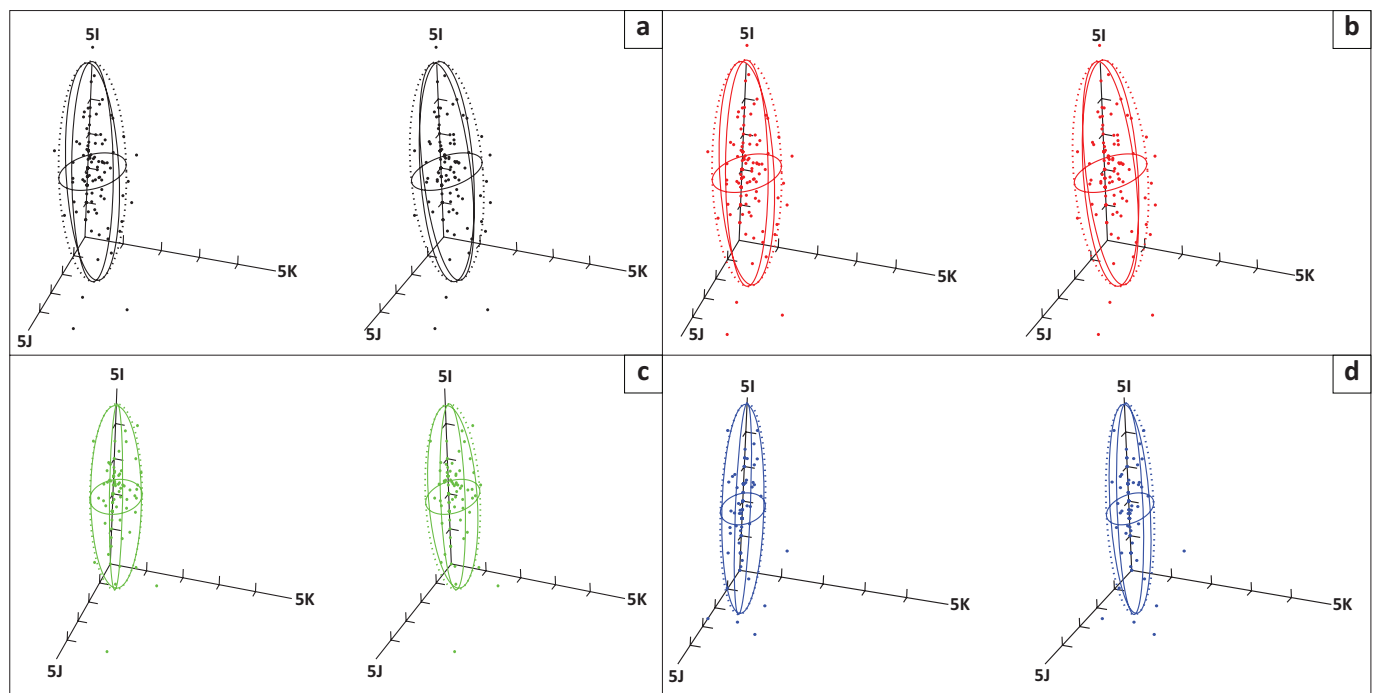


FIGURE 3: (a–d) Stereo-pair scatter plots with 95% distribution ellipsoids for near-refractive errors of presbyopic patients who were seen at the clinic in 2018 and 2019.

OS of presbyopic patients consulted at the clinic in 2018 and 2019. The 2018 sample includes 141 near-refractive errors, while the 2019 sample includes 110. The centroids of the CE and sample means shifted above the origin because of the proximal additions.

Figure 4 shows presbyopic samples for (Figure 4a) 2018 OD (black), (Figure 4b) 2018 OS (red), (Figure 4c) 2019 OD (green) and (Figure 4d) 2019 OS (blue) on the sample mean. In Figure 4a, b, c and d, the axis lengths for the above plots were set at 1I D to increase the visibility of the confidence ellipsoids with tick intervals of 0.25 D. The origin is OD throughout.

Figure 5 presents stereo-pair plots and distribution ellipsoids (as in Figure 1), rotated (0, -90°) for the near-refractive errors of 141 presbyopic patients from the 2018 sample and 110 patients from the 2019 sample. This rotation allows the viewer to observe the data along the stigmatic axis (labelled 2I), with the anti-stigmatic plane aligned with the plane of the page. This rotated view assists in assessing the cylindrical powers as part of the near-refractive states. The greater the cylinder power, the

farther a point is positioned from the stigmatic axis (emerging out of the plane of the page).

Figure 5a and b represent rotated ellipsoids for OD (black) and OS (red) in the 2018 sample, whereas (Figure 5c) and (Figure 5d) represent rotated ellipsoids for OD (green) and OS (blue) in the 2019 sample. The axis lengths are 2I D and origins are OD.

Discussion

The present study found that the near-refractive error data for the right (OD) and left (OS) eyes did not follow a normal distribution. Instead, the data exhibited mild positive and/or negative skewness, including a profound leptokurtosis. The data primarily exhibited stigmatic characteristics and revealed a hyperopic shift, which can be attributed to the positive optical additions prescribed for the correction of presbyopia. Importantly, the additions prescribed for OD and OS were consistent among the sample of presbyopic patients, ensuring that no patient received unequal additions. A few outliers were identified outside the distribution ellipsoids (Figure 3), though the overall variation largely maintained a stigmatic nature.

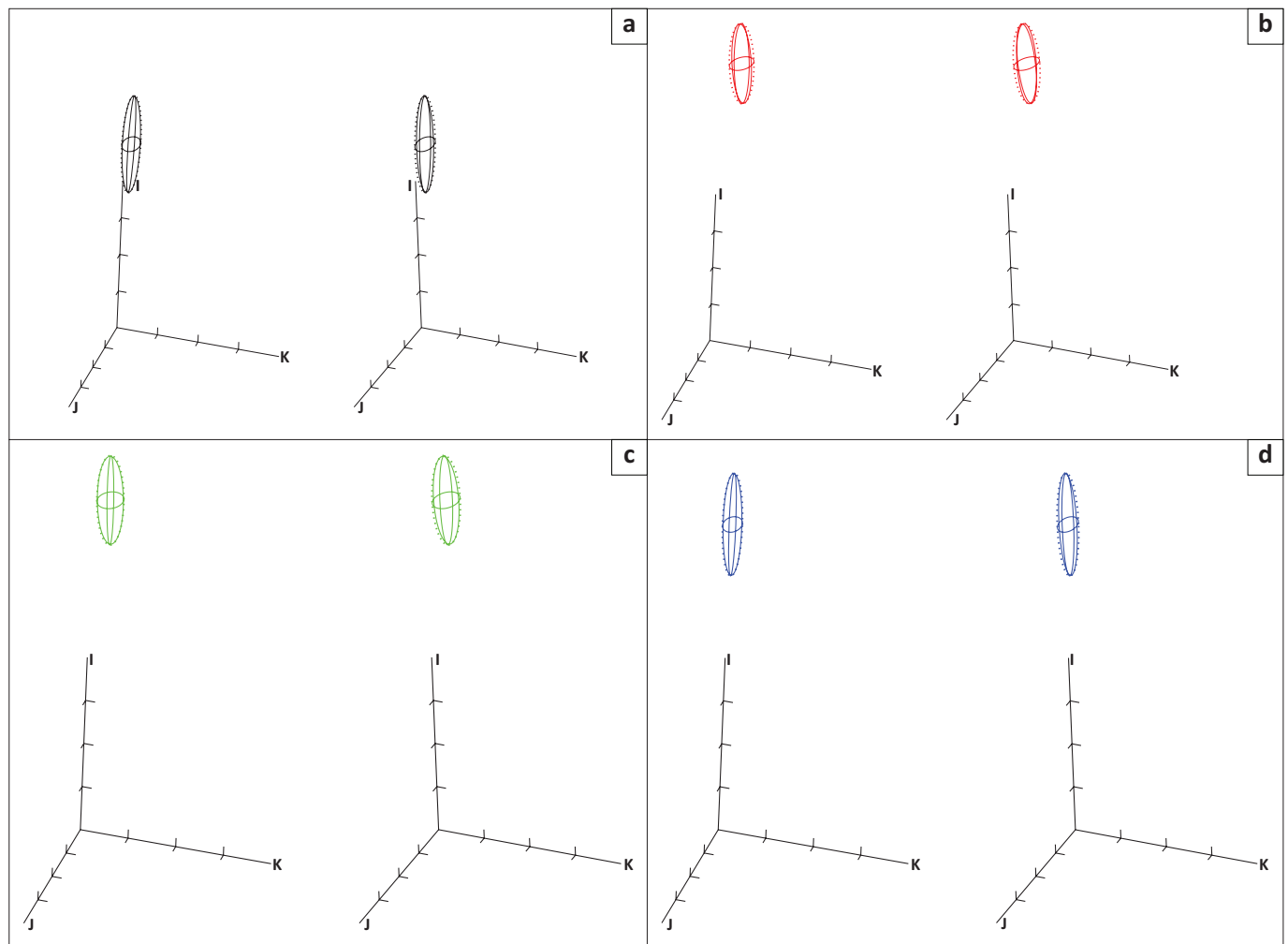


FIGURE 4: (a–d) Confidence ellipsoids (95%) on sample means of 141 near-refractive errors for OD and OS for presbyopic patients consulted at the clinic in 2018 and near-refractive errors ($N = 110$) for patients consulted at the clinic in 2019.

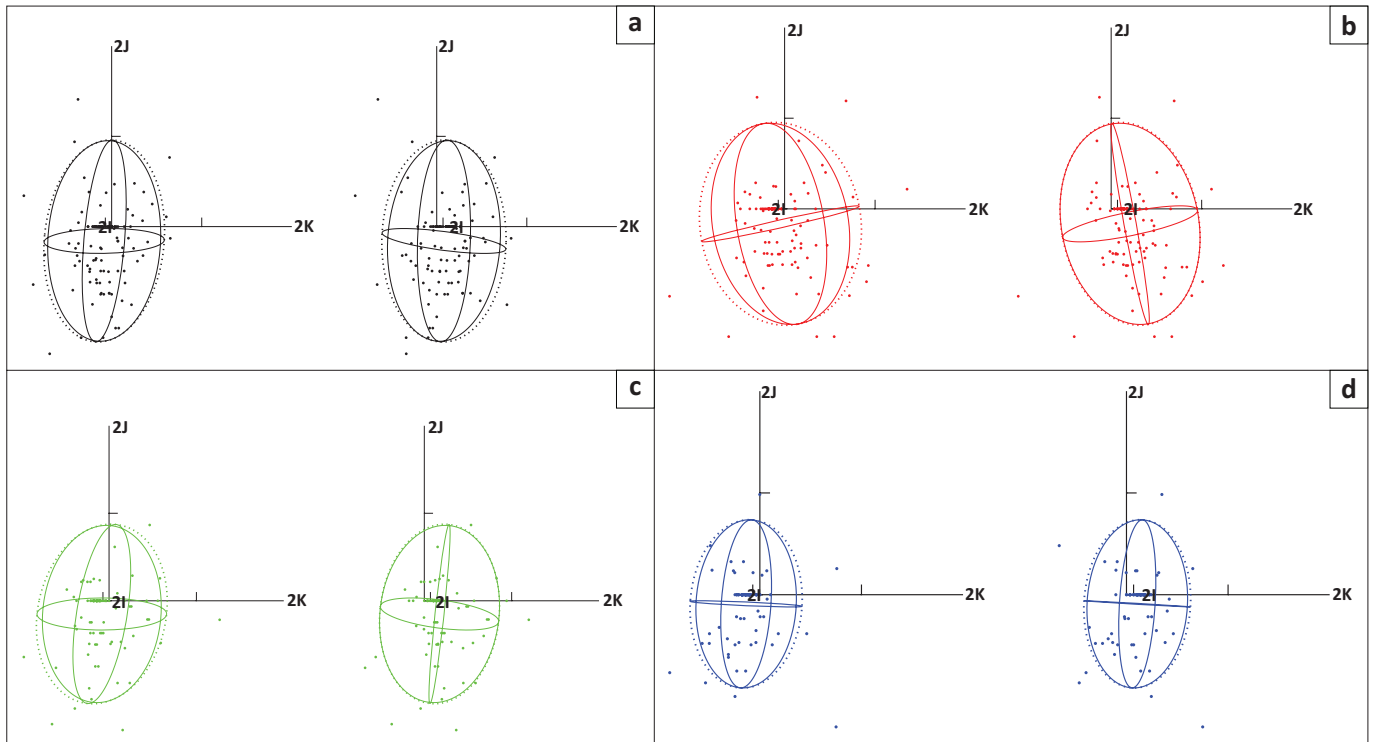


FIGURE 5: (a–d) Rotated ($0, -90^\circ$) stereo-pair scatter plots with 95% distribution ellipsoids for near-refractive errors for OD and OS of presbyopic patients.

This study serves as a follow-up to previous research conducted by Maluleke et al.²¹ concerning the distribution of non-cycloplegic subjective refractions at the Sekororo Hospital in Limpopo province, South Africa. While the earlier research primarily focussed on distance refraction samples, this study concentrates on near-refraction samples. The results presented here are comparable to the previous results of Hasrod¹⁸ and Unterhorst.³⁰ In this article, comparisons can easily be made regarding multivariate analysis methods such as meridional and stereo-pair plots used to analyse the near-refractive state for OD and OS. However, any comparisons should be cautiously approached because of differences in primary objectives, sample sizes, settings and research methodologies.

The sample size for the present study is larger (see Table 1) than that of Hasrod ($n = 21$) and is much larger than the Unterhorst sample ($n = 10$). The increased sample size in this hospital setting for the present study may be attributed to more attendees seeking routine eye care services, including treatments. While Unterhorst employed a cycloplegic autorefractometer procedure for data collection, the present study and Hasrod used non-cycloplegic subjective refraction methods. The meridional profiles for both OD and OS in the present study, and those from the previous studies, showed a non-symmetrical distribution of samples. In addition, variations across all studies were primarily stigmatic. Stereo-pair plots for OD and OS with 95% distribution ellipsoids indicated that the near-refractive data for presbyopic samples across all three studies exhibited a shift towards hyperopia.

A previous study by Fricke et al.¹ indicated that unaddressed presbyopia is associated with socioeconomic factors, particularly high levels of poverty and unemployment. This is especially true in developing and underdeveloped regions with limited access to eye care services, including inadequate provision of widely used optical aids like spectacles to address presbyopia. Similarly, the present study was conducted in a rural region facing the identified triple challenges (poverty, unemployment and inequality) in South Africa. As a result, affected individuals cannot afford common optical aids or corrections such as pair of spectacles causing an unaddressed high backlog in these regions.

Much variation in the near-refractive state was spherical (the stigmatic) irrespective of laterality or the year of consultation at the rural clinic involved. The rotated stereo-pair scatter plots ($0, -90^\circ$) presented in Figure 4 help identify anti-stigmatic variation in different orientations. Nonetheless, the near-refractive error data herein give useful information that can be used to understand the distribution of near-refractive error data for presbyopic patients who have undergone optometric care at the rural clinic involved. Again, it may also be useful for similar clinics in other parts of the world, especially for less-privileged regions where limitations in the availability of corrective lenses or spectacles for presbyopia and others might occasionally be a factor.

Possible limitations

The study had several limitations. It relied on retrospective data from only one of the five district hospitals in the Mopani District. The sample size was reduced because many records were excluded because of missing information. In addition,

the study's design and analytic methods could not establish causation. There was also a risk of biases, such as misclassification bias, wherein records with plus prescriptions might have been because of hyperopia rather than presbyopia. Furthermore, comparing the study's results was challenging because few previous studies employed multivariate analysis methods. As this research was conducted in a public hospital setting and gathered information from a single public optometrist, the findings cannot be generalised to private optometrists, the broader population or other levels of care, such as primary and tertiary settings.

Possible strengths

Multivariate analysis offers valuable insights into the distribution patterns and variability of the near-refractive states, particularly within African samples. The design of this study was time-efficient and minimised research costs, especially for materials like stationery used in interviewing participants. The large sample size in this study provides significant statistical power compared to the smaller sample sizes in previous studies conducted at other locations. The specialised software utilised in this research was particularly advantageous, as it could effectively analyse spherocylindrical prescriptions without the need to treat spheres, cylinders and their corresponding axes as separate entities. This analytical approach is widely recognised and understood across various scientific disciplines, including the engineering fraternity. The findings presented in this article may serve as a foundation for future research and enhance clinical decision-making based on these scientific discoveries, particularly regarding hyperopic shifts and additional factors.

Recommendations

The authors recommend that all undergraduate optometry programmes in South Africa and beyond incorporate multivariate analysis methods into their curricula. This integration will help future optometrists develop a deeper understanding of these techniques at the grassroots level. In addition, organisers of upcoming ophthalmic or optometric conferences and seminars should encourage submissions of more abstracts that utilise multivariate analysis, thereby enhancing participants' familiarity with these methods. It is also crucial for future ophthalmic studies to implement these advanced analytical techniques in their published research. Moreover, the distribution of near-vision addition lenses could be supported by any organisation or government willing to fund the purchase of simple reading spectacles to address presbyopia in the population.

Conclusion

The deviation from normality indicated that the near-refractive data for both the right and left eyes of presbyopic patients who visited the optometry clinic based at the district hospital concerned had a primarily mild positive skew across all meridians. The predominant variation in the refractive state for both eyes was spherical (stigmatic), irrespective of

the year of observation or laterality. Consequently, the distribution and variations in the near-refractive state of presbyopic patients were effectively achieved and analysed using the selected multivariate analysis methods.

Acknowledgements

Special acknowledgement is extended to the Provincial Health Research and Ethics Committee in the Limpopo Department of Health, the Senior Clinical Manager and the Chief Executive Officer of Sekororo Hospital for granting permission to conduct this study at their facility.

Competing interests

The authors declare that they have no financial or personal relationships that may have inappropriately influenced them in writing this article.

Authors' contributions

K.D.M., N.H. and A.R. contributed equally during the planning process and writing of this article. K.D.M. was the principal investigator of this study.

Funding information

This research received no specific grant from any funding agency in the public, commercial or not-for-profit sectors.

Data availability

The data that support the findings of this study are available on request from the corresponding author, K.D.M.

Disclaimer

The views and opinions expressed in this article are those of the authors and are the product of professional research. The article does not necessarily reflect the official policy or position of any affiliated institution, funder, agency or that of the publisher. The authors are responsible for this article's results, findings and content.

References

1. Fricke TR, Tahhan N, Resnikoff S, et al. Global prevalence of presbyopia and vision impairment from uncorrected presbyopia: Systematic review, meta-analysis, and modelling. *Ophthalmology*. 2018;125(10):1492–1499. <https://doi.org/10.1016/j.ophtha.2018.04.013>
2. American Optometric Association. Eye and vision conditions: Presbyopia [homepage on the Internet]. 2023 [cited 2023 Oct 08]. Available from: <https://www.who.int/>
3. American Academy of Ophthalmology. For public and patients: Eye health [homepage on the Internet]. 2023 [cited 2023 Oct 08]. Available from: <https://www.aao.org/>
4. World Health Organization. Eye care, vision impairment and blindness [homepage on the Internet]. 2023 [cited 2023 Oct 08]. Available from: <https://www.who.int/>
5. Uche JN, Ezegwui IR, Uche E, Onwasigwe EN, Umeh RE, Onwasigwe CN. Prevalence of presbyopia in a rural African community. *Rural Remote Health*. 2014;14:2731. <https://doi.org/10.22605/RRH2731>
6. Obajolowo TS, Owowe J, Adepoju FG. Prevalence and pattern of presbyopia in a rural Nigerian community. *J West Afr Coll Surg*. 2016;6(3):83–104.
7. Naidoo KS, Jaggernath J, Martin C, et al. Prevalence of presbyopia and spectacle coverage in an African population in Durban, South Africa. *Optom Vis Sci*. 2013;90(12):1427. <https://doi.org/10.1097/OPX.000000000000096>

8. Leshabane MM, Rampersad N, Mashige KP. Prevalence, causes, and factors associated with vision impairment in Limpopo Province. *Afr Vision Eye Health*. 2024;83(1):956. <https://doi.org/10.4102/aveh.v83i1.956>
9. Harris WF. The matrix representation of dioptric power. Part 1: An introduction. *S Afr Optomet*. 1988;47(4):19–23.
10. Keating MP. On the use of matrices for the mean value of refractive errors. *Ophthal Physiol Opt*. 1983;3(2):201–203. <https://doi.org/10.1111/j.1475-1333>
11. Saunders H. The algebra of spherocylinders. *Ophthal Physiol Opt*. 1985;5(2):157–163. [https://doi.org/10.1016/0275-5408\(85\)90069-9](https://doi.org/10.1016/0275-5408(85)90069-9)
12. Long WF. A matrix formalism for decentration problems. *Am J Optom Physiol Opt*. 1976;53:27–33. <https://doi.org/10.1097/00006324-197601000-00005>
13. Harris WF, Malan DJ, Rubin A. The distribution of dioptric power: Ellipsoids of constant probability density. *Ophthal Physiol Opt*. 1991;11(4):381–384. <https://doi.org/10.1111/j.1475-1313.1991.tb00239.x>
14. Harris WF. Representation of dioptric power in Euclidean 3-spaces. *Ophthal Physiol Opt*. 1991;11(2):130–136. <https://doi.org/10.1111/j.1475-1313.1991.tb00212.x>
15. Rubin A, Evans T, Hasrod N. Dioptric power and refractive behaviour: A review of methods and applications. *BMJ Open Ophthalmol*. 2022;7:e000929. <https://doi.org/10.1136/bmjophth-2021-000929>
16. Harris WF. Meridional profiles of variance-covariance of dioptric power. Part 1: The basic theory. *Ophthal Physiol Opt*. 1991;12(4):467–470. <https://doi.org/10.1111/j.1475-1313.1992.tb00317.x>
17. Harris WF, Malan DJ, Rubin A. Ellipsoidal confidence regions for mean refractive status. *Optom Vis Sci*. 1991;68(12):950–953. <https://doi.org/10.1097/00006324-199112000-00007>
18. Hasrod N. Intra- and intra-individual reliability of objective and subjective measures for determining the refractive state of the human eye [homepage on the Internet] [doctor of philosophy thesis (DPhil)]. Department of Optometry, University of Johannesburg: South Africa; 2022 [cited 2023 Nov 16]. Available from: <https://hdl.handle.net/10210/496944>
19. Thibos LN, Wheeler, W, Horner, D. Power vectors: An application of Fourier analysis to the description and statistical analysis of refractive error. *Optom Vis Sci*. 1997;74:367–375. <https://doi.org/10.1097/00006324-199706000-00019>
20. Statistics South Africa. Population: Limpopo Province [homepage on the Internet]. 2023 [cited 2023 Oct 10]. Available from: <https://www.statssa.gov.za>
21. Maluleke KD, Hasrod N, Rubin A. Distribution of noncycloplegic subjective refractions at Sekororo Hospital in Limpopo Province, South Africa. *Afr Vision Eye Health*. 2024;83(1):a892. <https://doi.org/10.4102/aveh.v83i1.892>
22. Cain MK, Zhang Z, Yuan KH. Univariate and multivariate skewness and kurtosis for measuring non-normality: Prevalence, influence, and estimation. *Behavior Research Methods*. 2016; 7(3):1–20. <https://doi.org/10.3758/s13428-016-0814-1>
23. Harris WF. Power vectors versus power matrices, and the mathematical nature of dioptric power. *Optom Vis Sci*. 2007;84:1060–1063. <https://doi.org/10.1097/OPX.0b013e318157acbb>
24. Chetty E, Rubin A. A review of multivariate methods of analysing refractive data with dioptric power matrices. *Afr Vision Eye Health*. 2022;81(1):a714. <https://doi.org/10.4102/aveh.v81i1.714>
25. Malan DJ. Computer programme for calculating mean refractive error. *S Afr Optomet*. 1990;49:83–85.
26. Malan DJ. Applying the dioptric power matrix: Computer programmes for practical calculations. *S Afr Optomet*. 1989;48:89–90.
27. Malan DJ. Dioptric power data analysis: Computer implementation of graphical methods with clinical examples. *S Afr Optomet*. 1993;52:84–90.
28. Chetty E. A multivariate analysis of short-term variation of keratometric behaviour, refractive state and pachymetry in keratoconus corneas [homepage on the Internet] [doctor of philosophy thesis (DPhil)]. Department of Optometry, University of Johannesburg: South Africa; 2019 [cited 2023 Dec 12]. Available from: <https://hdl.handle.net/102000/0002>
29. Moalusi SS. The relationship between autorefractometry, retinoscopy and subjective refraction by age [homepage on the Internet] [master of philosophy dissertation (MPhil)]. Department of Optometry: University of Johannesburg: South Africa; 1999 [cited 2023 Oct 13]. Available from: <https://hdl.handle.net/10210/6490>
30. Unterhorst HA. Multivariate analysis in symmetric dioptric power space of refractive state at two different distances, with and without cycloplegia [homepage on the Internet] [master of philosophy dissertation (MPhil)]. Department of Optometry: University of Johannesburg: South Africa; 2016 [cited 2023 Nov 19]. Available from: <https://hdl.handle.net/10210/91206>
31. Keating MP. A system matrix for the astigmatic optical system: Introduction and dioptric power relations. *Am J Optom Physiol Opt*. 1981;58(10):810–819. <https://doi.org/10.1097/00006324-19810000-00006>
32. Harris WF. Algebra of spherocylinders and refractive errors, and their means, variance, and standard deviation. *Am J Optom Physiol Opt*. 1988;65(10):794–802. <https://doi.org/10.1097/00006324-198810000-00003>
33. Harris WF. Simplified rational representation of dioptric power. *Ophthal Physiol Opt*. 1989;9(4):455. <https://doi.org/10.1111/j.1475-1313.1989.tb00952.x>
34. Keating MP. An easier method to obtain sphere, cylinder, and axis from an off-axis dioptric power matrix. *Am J Optom Physiol Opt*. 1980;57(10):734–737. <https://doi.org/10.1097/00006324-198010000-00007>
35. Harris WF. The matrix representation of dioptric power. Part 2: Adding obliquely crossed spherocylinders. *S Afr Optomet*. 1989;48:22–24.
36. Harris WF. The matrix representation of dioptric power. Part 3: The average refractive error. *S Afr Optomet*. 1989;48:81–88.